Differential brain activity in visuo-perceptual regions during landmark-based navigation in young and healthy older adults

Stephen Ramanoël[1,*,†], Marion Durteste[1,†], Marcia Bécu[1], Christophe Habas[2], Angelo Arleo[1]

[1] Sorbonne Université, INSERM, CNRS, Institut de la Vision, 17 rue Moreau, F-75012 Paris, France

[2] CHNO des Quinze-Vingts, DHU Sight Restore, INSERM-DHOS CIC, 28 rue de Charenton, 75012 Paris, France

Number of figures: 6

Number of tables: 5

[†] Co-first authorship

***CA, Corresponding Author**

Dr. Stephen Ramanoël,

mail: stephen.ramanoel@inserm.fr

Abstract

Older adults exhibit prominent impairments in their capacity to navigate, reorient in unfamiliar environments or update their path when faced with obstacles. This decline in navigational capabilities has traditionally been ascribed to memory impairments and dysexecutive function whereas the impact of visual aging has often been overlooked. The ability to perceive visuo-spatial information such as salient landmarks is essential to navigate in space efficiently. To date, the functional and neurobiological factors underpinning landmark processing in aging remain insufficiently characterized. To address this issue, this study used functional magnetic resonance imaging (fMRI) to investigate the brain activity associated with landmark-based navigation in young and healthy older participants. Twenty-five young adults (μ=25.4 years, σ=4.7; 7F) and twenty-one older adults (μ=73.0 years, σ=3.9; 10F) performed a virtual navigation task in the scanner in which they could only orient using salient landmarks. The underlying whole-brain patterns of activity as well as the functional roles of scene-selective regions, the parahippocampal place area (PPA), the occipital place area (OPA), and the retrosplenial cortex (RSC) were analyzed. We found that older adults' navigational abilities were diminished compared to young adults' and that the two age groups relied on distinct navigational strategies to solve the task. Better performance during landmark-based navigation was found to be associated with increased neural activity in an extended neural network comprising several cortical and cerebellar regions. Direct comparisons between age groups further revealed that young participants had enhanced anterior temporal activity. In addition, young adults only were found to recruit occipital areas corresponding to the cortical projection of the central visual field during landmark-based navigation. The region-of-interest analysis revealed increased OPA activation in older adult participants. There were no significant between-group differences in PPA and RSC activations. These results hint at the possibility that aging diminishes fine-grained information processing in occipital and temporal regions thus hindering the capacity to use landmarks adequately for navigation. This work helps towards a better comprehension of the neural dynamics subtending landmark-based navigation and it provides new insights on the impact of age-related visuo-spatial processing changes on navigation capabilities.

Key words: Healthy Aging, Spatial Navigation, Landmark, fMRI, scene-selective regions.

1. Introduction

Demographically, the 21st century is characterized by an unprecedented increase in the number of older adults within the worldwide population. There were 703 million people aged 65 years or over in 2019 and this number is projected to more than double by 2050 (United Nations, 2019). In parallel, we can expect a significant rise in the prevalence of neurodegenerative diseases such as Alzheimer's and Parkinson's diseases in the older population. In order to identify appropriate biomarkers, it is of critical importance that we gain a better understanding of brain changes in healthy aging. In this context, spatial navigation as a complex behavior encompassing perceptual and cognitive processes provides an ideal framework for the study of normal and pathological aging (Gazova et al., 2012; Lithfous et al., 2013; Allison et al., 2016; Laczo et al., 2017, 2018; Coughlan et al., 2018).

An extensive body of literature has highlighted a robust age-related decline in navigation ability in various species including rodents and non-human and human primates (Foster et al., 2012; Lester et al., 2017). Healthy older adults exhibit prominent impairments in their capacity to navigate efficiently, reorient or update their wayfinding behavior when faced with obstacles (Iaria et al., 2009; Moffat, 2009; Harris et al., 2012; Merhav et al., 2019). In real-world settings they are impaired at rapidly acquiring information about their surroundings leading to slower and more error-prone navigation than young adults (Kirasic, 1991; Wilkniss et al., 1997). In virtual reality (VR) paradigms older adults also choose inefficient routes, underestimate distances and make frequent turning errors (Adamo et al., 2012). Studies in VR have shed light on an age-related shift in the use of navigation strategies: older adults favor response over place-based strategies (Rodgers et al., 2012). A place-based strategy involves the formation of mental map-like representations of the absolute spatial position of the goal in relation to various stimuli within the environment. A response-based strategy refers to the process whereby an association between a specific stimulus and the goal location is formed. The choice of a navigation strategy critically depends on the visual information present in the environment (Foo et al., 2005; Ratliff and Newcombe, 2008). Indeed, successful navigation requires the perception and the integration of relevant spatial visual cues such as buildings or monuments, and the binding of these salient elements to directional information (Ekstrom, 2015; Epstein et al., 2017; Julian et al., 2018).

Spatial visual cues can be salient objects used as navigational landmarks or characteristics pertaining to the geometric shape of a space (Lester et al., 2017; Bécu et al., 2020). Landmarks can be conceptualized as discrete objects that are independent of the

environment's layout, such as a tree or a monument (Epstein and Vass, 2014). Landmarks' size, stability and proximity to the goal are among the key factors that influence their use for navigation (Stankiewicz and Kalia, 2007; Auger et al., 2012; Auger and Maguire, 2018). Geometric cues encompass all the elements that are intrinsic to and continuous with the external limits of a space; these include the overall layout, boundaries of the environment, wall lengths, and angle dimensions (Cheng and Newcombe, 2005; Tommasi et al., 2012; Giocomo, 2016). Several studies in virtual environments have emphasized the idea that old age hinders the ability to use landmark information for navigation (Picucci et al., 2009; Harris et al., 2012; Wiener et al., 2012; Zhong and Moffat, 2016; Hartmeyer et al., 2017). Bécu and colleagues (2020) recently elaborated on such results and unveiled a specific age-related deficit for landmark-based compared with geometry-based navigation in ecological settings. Older participants were found to be impaired in anchoring their spatial behavior to landmark information and relied preferentially on geometric cues when both types of visual spatial cues were informative.

Despite the extensive body of literature characterizing the neural underpinnings of human spatial navigation (for recent reviews see Chersi and Burgess, 2015; Spiers and Barry, 2015; Epstein et al., 2017; Herweg and Kahana, 2018; Julian et al., 2018), few experiments have explored this question in the context of healthy aging. Indeed, only fifteen peer-reviewed neuroimaging studies have focused on spatial processing in normal aging and the majority of these studies have used structural analyses (Li and King, 2019). These studies highlight an age-related decline in place-based navigation associated with structural and functional changes to the hippocampus. A unique fMRI study has investigated the link between the use of visual spatial cues and the navigational skills of young and older adults (Schuck et al., 2015a). The authors combined computational modeling and fMRI during a virtual navigation task to examine how participants learned object locations relative to a circular enclosure or to a salient landmark. Young participants were found to use a hippocampal-dependent system for the representation of geometry (circular arena) and a striatal-dependent system for the representation of a landmark (traffic cone). It was further revealed that older participants relied on hippocampal structures for landmark-based navigation and that they were insensitive to geometric information provided by the environmental boundaries. This absence of reliance on geometric information is surprising considering the behavioral findings mentioned above, and could be related to the small field of view inherent to the scanner (Sturz et al., 2013).

Several other brains regions, known to be altered in healthy aging (Lester et al., 2017; Zhong and Moffat, 2018), have also been identified as key for the processing of relevant visual spatial cues for navigation (Epstein and Vass, 2014; Julian et al., 2018). Recently, there has been growing interest in unearthing the roles of the parahippocampal place area (PPA), the occipital place area (OPA), and the retrosplenial cortex (RSC), regions that respond to the presentation of visual scenes such as landscapes or urban environments. These scene-selective areas have been speculated to integrate incoming visual inputs with higher-level cognitive processes (for a review see Epstein et al., 2017; Julian et al., 2018). In brief, the PPA is sensitive to navigationally relevant cues (Janzen and van Turennout, 2004; Epstein, 2008) and may be implicated in the recognition of spatial context (Marchette et al., 2015); the OPA has been associated with the processing of local elements in scenes (Kamps et al., 2016) as well as with the representation of environmental boundaries (Julian et al., 2016); and the RSC is suggested to anchor heading information to local visual cues (for a recent review of RSC functions see Mitchell et al., 2018). Research exploring the neural activity within scene-selective regions in the context of aging is still in its infancy but evidence is accumulating for age-related alterations in these regions. Functional changes in the PPA have been linked to deficient processing of visual scenes (Ramanoël et al., 2015) and lower activations in the RSC of older adults have been associated with difficulties in switching between navigation strategies (Zhong and Moffat, 2018). The OPA's progression as a function of age has not been fully characterized, but recent findings from the host laboratory have hinted at its preserved connectivity with other navigational brain structures in healthy aging (Ramanoël et al., 2019).

Although behavioral studies have provided some evidence for differences in the use of landmark cues across the lifespan, there is a clear paucity of research exploring the functional and neurobiological factors responsible for the deterioration of landmark information processing in older age. To address this caveat, the present study used fMRI to investigate to what extent healthy aging influences behavior and neural activity associated with landmark-based navigation. A second objective consisted in deciphering the role played by scene-selective regions (PPA, OPA, RSC) in age-related landmark-based navigation deficits.

2. Materials and methods

2.1 Participants

Among the 25 young adults and 21 older adults who completed the experiment, 4 older adults were excluded: 2 for a lack of task understanding and 2 for severe in-scanner

motion (movements > 5 mm across trials). Overall, 25 young adults (18 males; 25.4 ± 2.7 years) and 17 older adults (7 males; 73.0 ± 3.9 years) were included in the analyses. The participants were part of the French cohort study *SilverSight* (~350 subjects) established in 2015 at the Vision Institute, Quinze-Vingts National Ophthalmology Hospital, Paris. The battery of clinical and functional examinations used to enroll participants comprised an ophthalmological and functional visual screening, a neuropsychological evaluation, an oculomotor screening, an audio-vestibular assessment as well as a static/dynamic balance examination. The neuropsychological evaluation included the Mini Mental State Examination (MMSE; Folstein et al., 1975) and computerized versions of the 3D mental rotation test (Vandenberg and Kuse, 1978), perspective-taking test (Kozhevnikov and Hegarty, 2001) and Corsi block-tapping task (Corsi, 1973). Older participants had a score of 24[1] or higher on the MMSE. All subjects were right-handed, they had normal or corrected-to-normal vision, and they had no history of neurological or psychiatric disorders. Centration measurements and acuity were evaluated at least 2 weeks before the experimental session with a view to order MRI-compatible glasses for participants requiring visual correction (manufactured by *Essilor*). Participants gave their written informed consent to participate in the study, which was approved by the Ethical Committee "CPP Ile de France V" (ID_RCB 2015-A01094-45, CPP N°: 16122).

2.2 Virtual navigation task

2.2.1 The virtual environment

The virtual navigation task was displayed on a MRI-compatible liquid crystal display monitor (NordicNeuroLab, Bergen, Norway) positioned at the head of the scanner bore. Participants viewed the screen (size: 69.84 cm (H) x 39.26 cm (V); pixels: 1920 x 1080) at a distance of 115 cm via a mirror fixed above the head-coil. The visible part of the screen subtended approximately 34 x 20 degrees of visual angle.

The virtual environment was programmed with Unity3D game engine (Unity Technologies SF; San Francisco, CA; https://unity.com/) and had participants navigate actively in a first-person perspective. The virtual environment was a three-arm maze (Y-maze) consisting of three corridors radiating out from a center delimited by homogenous wooden-like walls. Two configurations were designed. In the landmark condition all arms

[1] All older participants scored 28 or above on the MMSE except one participant who scored 24. We decided to include this subject nonetheless as his extended neuropsychological evaluation was normal and no significant changes were detected when removing him from the fMRI analyses

were 18 virtual meters (vm) long and equiangular. Three light gray-colored objects (a square, a triangle and a circle) were placed in front of each short wall at the center of the maze (Figure 1-A). In the control condition, the arms were 18 vm long and equiangular, and the maze was devoid of objects (Figure 1-B).

Participants navigated actively through the virtual environment with an MRI-compatible ergonomic two-grip response device (NordicNeuroLab, Bergen, Norway). They could move forward (thumb press), turn right (right index press) and turn left (left index press). A single finger press was necessary to initiate or stop movement. The forward speed of movement was set at 3 vm/s and the turning speed at 40°/s.

2.2.2 Task design

Prior to scanning, all participants familiarized themselves with the response device in an unrelated virtual space both outside and inside the scanner. They were required to navigate within a square open-field environment and to walk over a wooden board that appeared at different locations.

The scanning session during the navigation task was divided into three runs: an encoding phase and a retrieval phase for the landmark condition and a control condition. At the start of the encoding phase participants were positioned in the center of the maze randomly facing one of the three arms. They were instructed to find a goal (gifts) hidden at the end of one corridor and remember its location using the visual information available in the center of the environment (the three light gray-colored objects). The encoding phase lasted 3 min to ensure that participants could explore all corridors. The retrieval phase in the same environment then began. In each trial participants were placed at the end of one of the two corridors that didn't contain the goal with their back against the wall. The starting positions across trials were pseudo-randomized across subjects. Participants were asked to navigate to the previously encoded goal location. Upon arrival at the end of the correct arm, the gifts appeared to indicate successful completion of the trial and a fixation cross on a gray screen was presented for an inter-trial interval of 3-8 s. Participants needed to complete seven trials. The control condition consisted of a retrieval phase only; it was designed to account for potential confounding factors such as motor and simple perceptual aspects of the task. It was always performed last and it comprised four trials. Subjects started from the end of an arm and moved to the center of the maze from where the target was readily visible. They were

instructed to navigate towards it. For both conditions, we recorded the trial duration and the response device use.

A short debriefing phase concluded the experimental session. Participants were probed on the strategy they used to orient in the landmark condition. They were asked to report how they solved the task: i) using one object, ii) using at least two objects, iii) randomly, iv) other strategy. Participants were deemed to be using a *place-based* strategy when their decision was based on two landmarks or more and to be using a *response-based* strategy when their decision was based on a single visual spatial cue (Iaria et al., 2003; Iglói et al., 2010, 2014; Chrastil, 2013; Gazova et al., 2013; Packard and Goodman, 2013; Colombo et al., 2017; Laczo et al., 2017). No participants answered that they oriented randomly or that they used a different strategy.

2.3 Functional localizer experiment

A block fMRI paradigm was used to locate scene-selective areas (Ramanoël et al., 2019). Scene-selective areas comprise the parahippocampal place area (PPA), the occipital place area (OPA) and the retrosplenial cortex (RSC). Participants were presented with blocks of 900 x 900 pixel grayscale photographs (18 x 18 degrees of visual angle) representing scenes, faces, everyday objects, and scrambled objects. The functional run lasted 4 min 40 s and it was composed of fourteen 20-s task blocks (4 blocks of scenes, 2 blocks of faces, 2 blocks of objects, 2 blocks of scrambled objects, and 4 blocks of fixation). Each stimulus was presented for 400 ms followed by a 600 ms inter-stimulus interval. Participants performed a "one-back" repetition detection task.

2.4 MRI Acquisition

Data were collected using a 3 Tesla Siemens MAGNETOM Skyra whole-body MRI system (Siemens Medical Solutions, Erlangen, Germany) equipped with a 64-channel head coil at the Quinze-Vingts National Ophthalmology Hospital in Paris, France. T2*-weighted echo-planar imaging (EPI) sequences, optimized to minimize signal dropout in the medial temporal region (Weiskopf et al., 2006), were acquired for functional imaging during the navigation task (voxel size = 3 x 3 x 2 mm, TR/TE/flip angle = 2685 ms/30 ms/90°, interslice gap = 1 mm, slices = 48, matrix size = 74 x 74, FOV = 220 x 220 mm). For the localizer experiment, 284 volumes from 64 slices were acquired using a T2*-weighted simultaneous multi-slice echo planar sequence (SMS-EPI; voxel size = 2.5 x 2.5 x 2.4 mm, TR/TE/flip

angle = 1000 ms/30 ms/90°, matrix size = 100 x 100, SMS = 2, GRAPPA = 2). The anatomical volume consisted of a T1-weighted, high-resolution three-dimensional MPRAGE sequence (voxel size = 1 x 1 x 1.2 mm, TR/TE/IT/flip angle = 2300 ms/2.9 ms/900 ms/9°, matrix size = 256 x 240 x 176).

2.5 Statistical analyses of behavioral data

Normality of data was assessed graphically with quantile-quantile plots and numerically with the Shapiro-Wilk test. Descriptive characteristics and cognitive measures were compared across age groups using independent samples t-test for normally distributed continuous data, Mann-Whitney U tests for non-normally distributed continuous data and chi-square test of independence for categorical data. Navigation performance (time to reach the goal, error rate) was compared across age group and sex with Mann-Whitney U tests. A logistic regression adjusted for sex was conducted to examine the relationship between age and strategy use in the landmark condition.

2.6 Preprocessing and statistical analyses of fMRI data

2.6.1 Whole brain analyses

FMRI data analysis was performed using a combination of SPM12 release 7487 (Wellcome Department of Imaging Neuroscience, London, UK) and ArtRepair toolbox (Mazaika et al., 2009) implemented in MATLAB 2015 (Mathworks Inc., Natick, MA, USA). The first five functional volumes of the encoding, retrieval and control runs were discarded to allow for equilibration effects. Slice-timing correction was applied and functional images were realigned to the mean functional image using a rigid body transformation. Artefacts related to motion were then examined with ArtRepair. Two older subjects were subsequently excluded. Volumes displaying elevated global intensity fluctuation (> 1.3%) and movement exceeding 0.5 mm/TR were repaired using interpolation from adjacent scans. The T1-weighted anatomical volume was then realigned to match the mean functional image of each participant and normalized to the Montreal Neurological Institute (MNI) space using a 4^{th} degree B-Spline interpolation. The anatomical normalization parameters were subsequently used for the normalization of functional volumes. Each functional scan was smoothed with an 8 mm FWHM (Full Width at Half Maximum) Gaussian kernel. The preprocessed images were visually inspected to ensure that there were no realignment or normalization issues.

Statistical analysis was performed using the general linear model for block design at the single participant level (Friston et al., 1995). The seven trials of the retrieval phase in the landmark condition, the four trials of the control condition and fixation times were modeled as regressors, constructed as box-car functions and convolved with the SPM hemodynamic response function (HRF). The encoding phase was not included in the analysis as its duration differed greatly between participants. Time to reach the goal by trial, grip response during navigation, and movement parameters derived from the realignment correction (three translations and three rotations) were entered in the design matrix as regressors of no-interest. Time series for each voxel were high-pass-filtered (1/128 Hz cutoff) to remove low-frequency noise and signal drift. Individual contrasts were submitted to a multiple regression and a two-samples t-test. Sex and total brain volume were included as covariates in the regression and total brain volume was included as a covariate in the two-samples t-test (see section 3.1). Areas of activation were tested for significance using a statistical threshold of $p < 0.001$ uncorrected at voxel-level, with a minimum cluster extent of k = 10 voxels (Iglói et al., 2010, 2014; Sutton et al., 2010; Schuck et al., 2015a; Javadi et al., 2017).

2.6.2 Region of interest analyses

Data from the localizer experiment were analyzed using SPM12. For each participant, the first 4 functional localizer volumes were discarded and the remaining images were realigned, co-registered to the T1-weighted anatomical image, normalized to the MNI space and smoothed using an 8 mm FWHM Gaussian kernel. Slice-timing correction was not applied following recommendations from the Human Connectome Project functional preprocessing pipeline for multi-slice sequences (Glasser et al., 2013). The localizer images were analyzed using a single participant general linear model for block design. Five conditions of interest (scenes, faces, objects, scrambled objects, fixation) were modeled as five regressors and convolved with a canonical HRF. Movement parameters were included in the model as regressors of no interest and each voxel's time-series was high-pass-filtered (1/128 Hz cutoff).

PPA, OPA and RSC regions were located independently for each participant using the fMRI contrast [Scenes > (Faces + Objects)]. Significant voxel clusters on individual t-maps were identified using family-wise error correction (FWE) for multiple comparisons (alpha = 0.05). Mask ROIs were created as the 40 contiguous voxels with the highest t-values around the peaks of activation from the left and right hemispheres. The two 40-voxel regions from

each hemisphere were subsequently summed into a single 80-voxel ROI. Mean parameter estimates for the contrast [Landmark > Control] were extracted from the three mapped ROIs using the REX MATLAB-based toolkit. The mean values from each ROI were compared between young and older subjects using two samples t-test and significance was set at $p < 0.0083$ after Bonferroni correction for multiple comparisons ($p = 0.05/(3 \times 2)$).

3. Results

3.1 Behavioral results

Data from 25 young and 17 older participants were analyzed. Neuropsychological assessments showed that older adults had significantly poorer performance than young adults across all measures. Descriptive and cognitive characteristics are summarized in Table 1.

Navigation performance across age groups is presented in Figure 2. We found that older adults chose the wrong corridor in 10% of trials while young adults made no errors (X^2 (1, N = 42) = 12.35, $p = 0.006$; Figure 2A). In addition, older subjects were significantly slower to reach the goal in the landmark condition than younger subjects (mean ± SEM: 19.85 s ± 1.67 vs 11.97 s ± 0.13; U(40) = 5.267, $p < 0.001$; Figure 2B). There was no sex effect on navigation time, defined by the average time to reach the goal, in each age group separately. However, when data from both age groups were pooled women's navigation time appeared to be significantly longer than men's (17.75 s ± 1.88 s vs 13.40 s ± 0.64 s; U(40) = 2.294, $p = 0.022$). Sex and total intracranial volume were therefore included as covariates in the fMRI multiple regression analyses. We further found that age was a significant predictor of strategy use ($R^2 = 0.967$, $p = 0.048$). Older adults were less likely to rely on a place-based strategy during landmark-based navigation than younger adults (Figure 2C).

3.2 Whole-brain

3.2.1 Multiple regression analyses

To locate the brain regions related to navigation performance, we first examined the association between both groups' navigation time and patterns of brain activity for the fMRI contrast [Landmark > Control]. We observed a negative association between navigation time and neural activity in many clusters across the brain (Table 2 and Figure 3) including frontal (right superior and middle gyri), temporal (middle, inferior, lingual and parahippocampal gyri), parietal (left angular gyrus including the inferior parietal lobule) and occipital cortices (left superior occipital gyrus) as well as in the cerebellum (lobule VI and vermis). Temporal

activations in the left hemisphere comprised the posterior part of the hippocampus: CA1 and the Dentate Gyrus (x=-24, y=-46, z=5 and x=-36, y=-43, z=-4). Other activations included the ventral temporal cortex (x=45, y=8, z=-37 and x=54, y=5, z=-34) and the visual area V3A (x=-21, y=-97, z=23) that is part of the dorsal visual stream. The inverse association did not elicit any significant brain activations. Complementary analyses revealed a negative association between age and patterns of neural activity in the left superior temporal gyrus only (x=-45, y=-1, z=-16) for the fMRI contrast [Landmark > Control]. The latter finding suggests that the negative association between navigation time and temporal activations previously reported is largely driven by age.

We then investigated the relationship between navigation time and neural activity in each age group separately (Table 2). In the young participant group, navigation performance was associated with neural activity in the left superior frontal gyrus and in the right precentral gyrus. In the older participant group, results revealed a main cluster in the left angular gyrus, including the inferior parietal lobule, as well as a small cluster encompassing the brainstem and the parahippocampal gyrus.

3.2.2 Two-sample analyses

Results for the within-group and between-group analyses are shown in Table 3 and Figure 4. We first contrasted brain activity during the landmark condition with activity during the control condition [Landmark > Control] for each age group individually. For young participants, we found significant clusters in the superior and inferior temporal gyri of the left hemisphere, which included the amygdala and hippocampus, in the middle and inferior occipital gyri bilaterally and in the right cerebellum (Crus I-II). In the older participant group, the fMRI contrast [Landmark > Control] did not elicit any significant activation. Direct comparisons between age groups revealed significant results for the fMRI contrast [Young > Old] but not for the contrast [Old > Young]. Young participants exhibited stronger activity in the left inferior temporal gyrus, comprising the amygdala and hippocampal regions, than older subjects.

The absence of activation in the older adult group prompted us to conduct further analyses. We first investigated the cognitive cost of the control condition in each age group by comparing cerebral activations for the fMRI contrast [Control > Fixation]. The group comparison [Young > Old] showed no significant activation. However, the inverse group comparison [Old > Young] revealed extended activations in the right precuneus, the right

superior temporal gyrus, the right supramarginal gyrus and superior parietal lobule as well as several bilateral frontal regions (Table 4). These results hint at the possibility that the control condition was cognitively more demanding for older participants than for young participants. We performed a second group comparison with the fMRI contrast [Landmark > Fixation] using a conservative cluster-level FWE correction $p < 0.05$. Significant activations were reported for the [Old > Young] comparison only, and included the middle frontal and superior parietal gyri in each hemisphere, the left supramarginal gyrus as well as the right cerebellum (Table 5).

3.3 Regions of interest

The PPA, OPA and RSC ROIs were defined for each individual based on the independent localizer experiment. We first examined age-related differences in average parameter activity for the fMRI contrast [Landmark > Control]. No significant differences were found. We conducted a second analysis based on the fMRI contrast [Landmark > Fixation]. The group comparison revealed significantly enhanced OPA activity in older adults compared with young adults after adjusting for multiple comparisons (mean ± SEM: 2.19 ± 0.27 vs. 1.07 ± 0.21; t = -3.4, $p = 0.002$). No significant differences were observed in the activity of the PPA and RSC between young and older participants (Figure 5).

4. Discussion

The present fMRI study examined age-related differences in landmark-based navigation using a non-ambiguous Y-maze reorientation paradigm. The task was designed to limit the influence of mnemonic and motor components in order to gain a specific understanding of the neural bases subtending visual spatial cue reliance in young and healthy older adults.

Behavior

We first replicated well-established findings and showed that older adults had lower scores than their younger counterparts on visuo-spatial cognitive neuropsychological measures, including the perspective-taking, 3D mental rotation and Corsi block-tapping tasks (Ohta et al., 1981; Clancy Dollinger, 1995; Iachini et al., 2005; Techentin et al., 2014). These tests are known to be good predictors of general navigation skills and their decline with age may account in part for older adults' deficient navigation performance (Zhong and Moffat, 2016). Notably, perspective-taking, mental rotation, and spatial memory are important

abilities for spatial learning and for the dynamic manipulation of sensory information during navigation (Allen et al., 1996; Kozhevnikov et al., 2006; Meneghetti et al., 2018; Muffato et al., 2020).

Consistent with past literature, we found that older subjects' navigation performance was significantly poorer than young subjects' and we reported a bias for response-based strategies in older adults (Moffat and Resnick, 2002; Harris and Wolbers, 2012; Rodgers et al., 2012; Gazova et al., 2013; Wiener et al., 2013; Schuck et al., 2015b; van der Ham et al., 2015; Zhong and Moffat, 2016; Kimura et al., 2019; Merhav and Wolbers, 2019; Bécu et al., 2020). This navigation strategy preference appeared to be associated with older age. However, we cannot exclude the possibility that the differential proportion of women in the two age groups (young: 28% vs. old: 59%) partly accounted for the increased use of response-based strategies in older adults (Perrochon et al., 2018). Notwithstanding these age-related differences, it is important to mention that older participants achieved a high level of performance on the task and made few errors. We argue that this result stemmed from the simplicity of the virtual environment that contained a unique junction and three proximal landmarks (Moffat and Resnick, 2002; Caffo et al., 2018). Moreover, both place- and response-based strategies could be used to successfully complete the task.

Whole-brain

In accordance with previous neuroimaging studies looking at the neural bases of spatial navigation, we found that landmark-based navigation recruited an extended network of brain regions (Kuhn and Gallinat, 2014; Spiers and Barry, 2015b; Coughlan et al., 2018; Cona and Scarpazza, 2019).

This network spanned posterior structures linked to visuo-spatial processing. We reported activation of the left superior occipital gyrus which corresponds to visual area V3A and is involved in optic flow tracking for visual path integration (Sherrill et al., 2015; Zajac et al., 2019). In addition, our landmark-based navigation paradigm elicited activity in the ventral temporal cortex. The latter is known to process high-level visual information such as object quality (Kravitz et al., 2013; Nau et al., 2018). The recruited network also encompassed the posterior section of the hippocampus and the parahippocampal gyrus; brain areas that play a central role in spatial navigation and that are particularly active during immediate retrieval phases of navigation paradigms (Kuhn and Gallinat, 2014; Cona and Scarpazza, 2019). Furthermore, we found significant activity in the angular gyrus, a region of the posterior

parietal cortex known to encode landmarks in the environment with respect to the self (Ciaramelli et al., 2010; Auger and Maguire, 2018). Our task also prompted activation of the prefrontal cortex which is thought to contribute to spatial working memory during active navigation (Wolbers and Hegarty, 2010; Ito, 2018). It thus appears that accurate landmark-based navigation required the integration of objects within a first-person framework and the maintenance of such representations in working memory (Sack, 2009; Seghier, 2012; Miniaci and De Leonibus, 2018). Finally, we found that lobule VI and the vermis of the right cerebellum were active during landmark-based navigation. This finding is in accordance with the cerebellum's postulated role in cognitive aspects of spatial navigation (Rochefort et al., 2013). We must nonetheless acknowledge the eventuality that cerebellar activity reflected sensory-motor processing such as the degree of motor learning or eye and finger movements (Bo et al., 2011; Igloi et al., 2015).

Importantly, older participants were found to over-recruit superior parietal regions compared to young participants. One could speculate that the increased bilateral activity in the angular gyrus drove the encoding of landmarks in a first-person perspective leading to a bias for response strategies in the older adult group. This is consistent with the observed age-related reduction in temporal activity. Indeed, changes in strategy preference with advancing age have been extensively documented and they are thought to be mediated by a shift from the hippocampal regions towards other cerebral structures such as the parietal cortex (Rodgers et al., 2012; Wiener et al., 2013). Within this framework of interpretation, older adults' increased cerebellar activity could also reflect a change in strategy preference as recent evidence has implicated the cerebellum in the mediation of response-based strategies (Igloi et al., 2015). Older participants further displayed enhanced activation of frontal cortices. Various authors have stressed the impact of age-related modifications in the prefrontal cortex on hippocampal and striatal dynamics, which could contribute to impaired strategy implementation and switching (Lester et al., 2017; Goodroe et al., 2018; Zhong and Moffat, 2018). In contrast to previous studies that reported striatal activity during response-based navigation, our results did not show increased striatal activity in the older adult group (Konishi et al., 2013; Schuck et al., 2015b). Such a difference may be explained by the high proportion of young adults using response-based strategies in our task. Worthy of note, the differential patterns of neural activity observed in the young and older participant groups may be partially due to age-related cognitive and motor differences. Although we tailored the duration of the familiarization phase to each subject's needs and controlled for response

device use, we cannot omit the potential influence of older adults' lesser familiarity with new technologies and declining executive functions. For example, the lack of activity elicited by the contrast [Landmark > Control] in older subjects could reflect the deficient integration of new instructions when switching between tasks (Hirsch et al., 2016).

Of interest, whole-brain analyses revealed that young adults recruited the cortical projections of the central visual field in posterior occipital regions (Figure 6, MNI coordinates left: x=-24, y=-49, z=2 and right: x=30, y=-49, z=2). The latter brain area is dedicated to fine-grained visual perception such as object recognition (Wandell et al., 2005; Kauffmann et al., 2014). Exploratory between-group analyses showed that the fMRI contrast [Landmark] elicited more activity in anterior occipital regions (MNI coordinates x=6, y=-73, z=-1) that respond to the peripheral visual field in older participants than in young participants (Figure 6). Previous neuroimaging studies have uncovered specific age-related changes in the occipital regions associated with central visual field processing and a relative preservation of areas associated with peripheral visual field processing (Brewer and Barton, 2012; Ramanoël et al., 2015). Additionally, group comparisons revealed that young subjects had more activity in the anterior section of the inferior temporal gyrus than older subjects. As mentioned previously, the anterior temporal cortex is critical for perceptual recognition and visual object processing (Litman et al., 2009). Our findings are therefore consistent with recent evidence highlighting deficient fine-grained processing of sensory information in older adults and emphasize the importance of acute object discrimination for landmark-based navigation and episodic memory (Burke et al., 2018; Greene and Naveh-Benjamin, 2020). Taken together, the above results suggest that occipital and temporal regions involved in the representation of fine-grained information are particularly disrupted in older age. Further research is warranted to determine whether the age-related decline in orientation skills could stem from the less efficient processing of visual spatial cues.

Scene-selective regions

Given the predominant role of visual perception in human spatial navigation (Ekstrom, 2015; Nau et al., 2018), there has been heightened interest in the PPA, RSC and OPA and their respective contributions to landmark processing (Epstein et al., 2017; Julian et al., 2018). Our results pointed to greater OPA activity in older participants compared with younger participants which is in line with recent work showing a higher functional connectivity around the OPA in older adults (Ramanoël et al., 2019).The OPA is known to be sensitive to self-perceived distance and motion (Persichetti and Dilks, 2016) and to extract the navigational

affordances of the local visual scene from a first-person perspective (Bonner and Epstein, 2017). Critically, these self-centered navigation skills are relatively well preserved in healthy aging (Moffat, 2009). In line with the over-activation of the parietal cortex in older adults, one could conceive that the increased OPA activation in the older adult group reflects a compensatory mechanism to offset the reduced activity in the temporal cortex, thus mitigating age-related place learning deficits. As a side note, considering that the OPA has been causally linked to the processing of environmental boundaries (Julian et al., 2016), our result offers a potential explanation for older adults' preferential reliance on geometric information in an ecological cue conflict paradigm (Bécu et al., 2020).

Surprisingly, we did not find differences in the activity of the RSC across age groups. Previous work has demonstrated an age-related decline in RSC activation during spatial navigation tasks (Meulenbroek et al., 2004; Moffat et al., 2006; Antonova et al., 2009). The RSC is known to mediate several cognitive functions pertaining to spatial navigation (Vann et al., 2009; Mitchell et al., 2018) including translation between reference frames and recollection of visual landmarks (Auger et al., 2015). The discrepancy between our results and those from the literature could be explained by the relative simplicity of our task. In contrast to previous research conducted with young adults, our paradigm strived to restrict mnemonic processing and comprised only three stable, salient and simple landmarks located at a single intersection (Wolbers and Büchel, 2005; Auger et al., 2012; Auger and Maguire, 2018). Another probable explanation lies in the idea that functional and structural changes to the RSC have been proposed to be more pronounced in pathological aging than normal aging (Fjell et al., 2014; Dillen et al., 2016).

Finally, we reported a weak recruitment of the PPA during landmark-based navigation with no significant difference across age groups. Previous studies have found the PPA to be involved in encoding the navigational relevance of objects for orientation (Janzen and van Turennout, 2004) and in landmark recognition (Epstein and Vass, 2014). As previously noted, our virtual environment comprised a small number of simple and non-ambiguous objects, the lack of activity in the PPA is thus unsurprising. In addition, two recent studies de-emphasized PPA's contribution to active navigation and highlighted its specificity for place recognition (Persichetti and Dilks, 2018, 2019). Research exploring the neural activity within scene-selective regions in the context of aging is still in its infancy. Future studies are needed to better characterize age-related changes in brain areas implicated in processing both the visual and cognitive properties of spatial cues.

Limitations

The current study has several limitations. First, we focused exclusively on the retrieval phase as the encoding phase proved to be too heterogeneous across participants. It would be of immediate interest to assess the influence of various visuo-perceptual modulations, such as the visibility of spatial cues, on the quality of spatial encoding. Second, although spatial navigation is reliant upon multiple sources of sensory information, fMRI spatial navigation paradigms only allow for visual input signals. Active walking as part of ecological study designs would provide proprioceptive and self-motion feedback signals as well as an improved field of view to participants. Such studies are necessary to complement the present findings. Previous research has indeed shown that navigation performance in older subjects is tightly coupled to the availability of multiple sources of sensory information (Adamo et al., 2012). Finally, future studies should take into consideration the role of sex and should include an intermediate age group in order to gain a finer understanding of the neural dynamics subtending spatial navigation across the lifespan (Grön et al., 2000; van der Ham and Claessen, 2020).

5. Conclusion

To conclude, the present study shed light on the possibility that navigational deficits in old age are linked to functional differences in brain areas involved in visual processing and to impaired representations of landmarks in temporal regions. This work helps towards a better comprehension of the neural dynamics subtending landmark-based navigation and it provides new insights on the impact of age-related spatial processing changes on navigation capabilities. We argue that approaching the study of spatial navigation in healthy and pathological aging from the perspective of visuo-perceptual abilities is a critical next step in the field. Neuroimaging methods coupled with virtual reality paradigms open up promising avenues to investigate age-related changes in navigation ability and to evaluate the benefits of training programs on older adults' spatial autonomy and mobility.

Author Contributions

Study design: SR, MB, CH, AA; Data acquisition: SR, MD; Data processing: SR, MD; Manuscript writing: SR, MD, MB, AA.

Conflict of Interest Statement

The authors declare that the research was conducted in the absence of any commercial or financial relationships that could be construed as a potential conflict of interest.

Funding

This research was supported by ANR – Essilor SilverSight Chair ANR-14-CHIN-0001.

Acknowledgments

The authors would like to express their gratitude to the men and women who took part in this study. We thank the Quinze-Vingts Hospital for allowing us to acquire the MRI data. We thank Konogan Baranton and Isabelle Poulain (*Essilor*) for the manufacturing of MRI-compatible glasses.

Bibliography

Adamo, D. E., Brice??o, E. M., Sindone, J. A., Alexander, N. B., and Moffat, S. D. (2012). Age differences in virtual environment and real world path integration. *Front. Aging Neurosci.* 4, 1–9. doi:10.3389/fnagi.2012.00026.

Allen, G. L., Kirasic, K. C., Dobson, S. H., Long, R. G., and Beck, S. (1996). Predicting environmental learning from spatial abilities: An indirect route. *Intelligence* 22, 327–355. doi:https://doi.org/10.1016/S0160-2896(96)90026-4.

Allison, S. L., Fagan, A. M., Morris, J. C., and Head, D. (2016). Spatial Navigation in Preclinical Alzheimer's Disease. *J. Alzheimers. Dis.* 52, 77–90. doi:10.3233/JAD-150855.

Antonova, E., Parslow, D., Brammer, M., Dawson, G. R., Jackson, S. H. D., and Morris, R. G. (2009). Age-related neural activity during allocentric spatial memory. *Memory* 17, 125–143. doi:10.1080/09658210802077348.

Auger, S. D., and Maguire, E. A. (2018). Retrosplenial Cortex Indexes Stability beyond the Spatial Domain. *J. Neurosci.* 38, 1472–1481. doi:10.1523/JNEUROSCI.2602-17.2017.

Auger, S. D., Mullally, S. L., and Maguire, E. A. (2012). Retrosplenial cortex codes for permanent landmarks. *PLoS One* 7. doi:10.1371/journal.pone.0043620.

Auger, S. D., Zeidman, P., and Maguire, E. A. (2015). A central role for the retrosplenial

577 cortex in de novo environmental learning. *Elife* 4, 1–26. doi:10.7554/eLife.09031.

578 Bécu, M., Sheynikhovich, D., Tatur, G., Agathos, C. P., Bologna, L. L., Sahel, J.-A., et al.
579 (2020). Age-related preference for geometric spatial cues during real-world navigation.
580 *Nat. Hum. Behav.* 4, 88–99. doi:10.1038/s41562-019-0718-z.

581 Bo, J., Peltier, S. J., Noll, D. C., and Seidler, R. D. (2011). Age differences in symbolic
582 representations of motor sequence learning. *Neurosci. Lett.* 504, 68–72.
583 doi:10.1016/j.neulet.2011.08.060.

584 Bonner, M. F., and Epstein, R. A. (2017). Coding of navigational affordances in the human
585 visual system. *Proc. Natl. Acad. Sci. U. S. A.* 114, 4793–4798.
586 doi:10.1073/pnas.1618228114.

587 Brewer, A. a., and Barton, B. (2012). Effects of healthy aging on human primary visual
588 cortex. *Health (Irvine. Calif).* 04, 695–702. doi:10.4236/health.2012.429109.

589 Burke, S. N., Gaynor, L. S., Barnes, C. A., Bauer, R. M., Bizon, J. L., Roberson, E. D., et al.
590 (2018). Shared Functions of Perirhinal and Parahippocampal Cortices: Implications for
591 Cognitive Aging. *Trends Neurosci.* 41, 349–359. doi:10.1016/J.TINS.2018.03.001.

592 Caffo, A. O., Lopez, A., Spano, G., Serino, S., Cipresso, P., Stasolla, F., et al. (2018). Spatial
593 reorientation decline in aging: the combination of geometry and landmarks. *Aging Ment.*
594 *Health* 22, 1372–1383. doi:10.1080/13607863.2017.1354973.

595 Cheng, K., and Newcombe, N. S. (2005). Is there a geometric module for spatial orientation?
596 Squaring theory and evidence. *Psychon. Bull. Rev.* 12, 1–23. doi:10.3758/BF03196346.

597 Chersi, F., and Burgess, N. (2015). The Cognitive Architecture of Spatial Navigation:
598 Hippocampal and Striatal Contributions. *Neuron* 88, 64–77.
599 doi:10.1016/j.neuron.2015.09.021.

600 Chrastil, E. R. (2013). Neural evidence supports a novel framework for spatial navigation.
601 *Psychon. Bull. Rev.* 20, 208–27. doi:10.3758/s13423-012-0351-6.

602 Ciaramelli, E., Rosenbaum, R. S., Solcz, S., Levine, B., and Moscovitch, M. (2010). Mental
603 space travel: damage to posterior parietal cortex prevents egocentric navigation and
604 reexperiencing of remote spatial memories. *J. Exp. Psychol. Learn. Mem. Cogn.* 36,
605 619–634. doi:10.1037/a0019181.

606 Clancy Dollinger, S. M. (1995). Mental rotation performance: Age, sex, and visual field
607 differences. *Dev. Neuropsychol.* 11, 215–222. doi:10.1080/87565649509540614.

608 Colombo, D., Serino, S., Tuena, C., Pedroli, E., Dakanalis, A., Cipresso, P., et al. (2017).
609 Egocentric and allocentric spatial reference frames in aging: A systematic review.
610 *Neurosci. Biobehav. Rev.* 80, 605–621. doi:10.1016/j.neubiorev.2017.07.012.

611 Cona, G., and Scarpazza, C. (2019). Where is the "where" in the brain? A meta-analysis of
612 neuroimaging studies on spatial cognition. *Hum. Brain Mapp.* 40, 1867–1886.
613 doi:10.1002/hbm.24496.

614 Corsi, P. M. (1973). Human memory and the medial temporal region of the brain. 34.

615 Coughlan, G., Laczo, J., Hort, J., Minihane, A.-M., and Hornberger, M. (2018). Spatial
616 navigation deficits - overlooked cognitive marker for preclinical Alzheimer disease? *Nat.*
617 *Rev. Neurol.* 14, 496–506. doi:10.1038/s41582-018-0031-x.

618 Dillen, K. N. H., Jacobs, H. I. L., Kukolja, J., von Reutern, B., Richter, N., Onur, Ö. A., et al.
619 (2016). Aberrant functional connectivity differentiates retrosplenial cortex from posterior
620 cingulate cortex in prodromal Alzheimer's disease. *Neurobiol. Aging* 44, 114–126.
621 doi:https://doi.org/10.1016/j.neurobiolaging.2016.04.010.

622 Ekstrom, A. D. (2015). Why vision is important to how we navigate. *Hippocampus* 25, 731–
623 735. doi:10.1002/hipo.22449.

624 Epstein, R. A. (2008). Parahippocampal and retrosplenial contributions to human spatial
625 navigation. *Trends Cogn. Sci.* 12, 388–396. doi:10.1016/j.tics.2008.07.004.

626 Epstein, R. A., Patai, E. Z., Julian, J. B., and Spiers, H. J. (2017). The cognitive map in
627 humans: spatial navigation and beyond. *Nat. Neurosci.* 20, 1504–1513.
628 doi:10.1038/nn.4656.

629 Epstein, R. a, and Vass, L. K. (2014). Neural systems for landmark-based wayfinding in
630 humans. *Philos. Trans. R. Soc. Lond. B. Biol. Sci.* 369, 20120533.
631 doi:10.1098/rstb.2012.0533.

632 Fjell, A. M., McEvoy, L., Holland, D., Dale, A. M., and Walhovd, K. B. (2014). What is
633 normal in normal aging? Effects of aging, amyloid and Alzheimer's disease on the
634 cerebral cortex and the hippocampus. *Prog. Neurobiol.* 117, 20–40.

635 doi:10.1016/j.pneurobio.2014.02.004.

636 Folstein, M. F., Folstein, S. E., and McHugh, P. R. (1975). “Mini-mental state”. A practical
637 method for grading the cognitive state of patients for the clinician. *J. Psychiatr. Res.* 12,
638 189–198.

639 Foo, P., Warren, W. H., Duchon, A., and Tarr, M. J. (2005). Do humans integrate routes into a
640 cognitive map? Map- versus landmark-based navigation of novel shortcuts. *J. Exp.*
641 *Psychol. Learn. Mem. Cogn.* 31, 195–215. doi:10.1037/0278-7393.31.2.195.

642 Foster, T. C., Defazio, R. A., and Bizon, J. L. (2012). Characterizing cognitive aging of
643 spatial and contextual memory in animal models. *Front. Aging Neurosci.* 4, 12.
644 doi:10.3389/fnagi.2012.00012.

645 Friston, K. J., Holmes, A. P., Worsley, K. J., Poline, J. P., Frith, C. D., and Frackowiak, R. S.
646 J. (1995). Statistical parametric maps in functional imaging: a general linear approach.
647 *Hum. Brain Mapp.* 2, 189–210.

648 Gazova, I., Laczó, J., Rubinova, E., Mokrisova, I., Hyncicova, E., Andel, R., et al. (2013).
649 Spatial navigation in young versus older adults. *Front. Aging Neurosci.* 5, 94.
650 doi:10.3389/fnagi.2013.00094.

651 Gazova, I., Vlcek, K., Laczó, J., Nedelska, Z., Hyncicova, E., Mokrisova, I., et al. (2012).
652 Spatial navigation—a unique window into physiological and pathological aging. *Front.*
653 *Aging Neurosci.* 4, 16. doi:10.3389/fnagi.2012.00016.

654 Giocomo, L. M. (2016). Environmental boundaries as a mechanism for correcting and
655 anchoring spatial maps. *J. Physiol.* 594, 6501–6511. doi:10.1113/JP270624.

656 Glasser, M. F., Sotiropoulos, S. N., Wilson, J. A., Coalson, T. S., Fischl, B., Andersson, J. L.,
657 et al. (2013). The minimal preprocessing pipelines for the Human Connectome Project.
658 *Neuroimage* 80, 105–124. doi:10.1016/j.neuroimage.2013.04.127.

659 Goodroe, S. C., Starnes, J., and Brown, T. I. (2018). The Complex Nature of Hippocampal-
660 Striatal Interactions in Spatial Navigation. *Front. Hum. Neurosci.* 12, 250.
661 doi:10.3389/fnhum.2018.00250.

662 Greene, N. R., and Naveh-Benjamin, M. (2020). A Specificity Principle of Memory: Evidence
663 From Aging and Associative Memory. *Psychol. Sci.*, 0956797620901760.

664 doi:10.1177/0956797620901760.

665 Grön, G., Wunderlich, a P., Spitzer, M., Tomczak, R., and Riepe, M. W. (2000). Brain
666 activation during human navigation: gender-different neural networks as substrate of
667 performance. *Nat. Neurosci.* 3, 404–8. doi:10.1038/73980.

668 Harris, M. A., Wiener, J. M., and Wolbers, T. (2012). Aging specifically impairs switching to
669 an allocentric navigational strategy. *Front. Aging Neurosci.* 4, 1–9.
670 doi:10.3389/fnagi.2012.00029.

671 Harris, M. A., and Wolbers, T. (2012). Ageing effects on path integration and landmark
672 navigation. *Hippocampus* 22, 1770–1780. doi:10.1002/hipo.22011.

673 Hartmeyer, S., Grzeschik, R., Wolbers, T., and Wiener, J. M. (2017). The Effects of
674 Attentional Engagement on Route Learning Performance in a Virtual Environment: An
675 Aging Study . *Front. Aging Neurosci.* 9, 235. Available at:
676 https://www.frontiersin.org/article/10.3389/fnagi.2017.00235.

677 Herweg, N. A., and Kahana, M. J. (2018). Spatial Representations in the Human Brain. *Front.*
678 *Hum. Neurosci.* 12, 297. doi:10.3389/fnhum.2018.00297.

679 Hirsch, P., Schwarzkopp, T., Declerck, M., Reese, S., and Koch, I. (2016). Age-related
680 differences in task switching and task preparation: Exploring the role of task-set
681 competition. *Acta Psychol. (Amst).* doi:10.1016/j.actpsy.2016.06.008.

682 Iachini, T., Poderico, C., Ruggiero, G., and Iavarone, A. (2005). Age differences in mental
683 scanning of locomotor maps. *Disabil. Rehabil.* 27, 741–752.
684 doi:10.1080/09638280400014782.

685 Iaria, G., Palermo, L., Committeri, G., and Barton, J. J. S. (2009). Age differences in the
686 formation and use of cognitive maps. *Behav. Brain Res.* 196, 187–191.
687 doi:10.1016/j.bbr.2008.08.040.

688 Iaria, G., Petrides, M., Dagher, A., Pike, B., and Bohbot, V. D. (2003). Cognitive strategies
689 dependent on the hippocampus and caudate nucleus in human navigation: variability and
690 change with practice. *J. Neurosci.* 23, 5945–5952. doi:23/13/5945 [pii].

691 Igloi, K., Doeller, C. F., Berthoz, A., Rondi-Reig, L., and Burgess, N. (2010). Lateralized
692 human hippocampal activity predicts navigation based on sequence or place memory.

693 *Proc. Natl. Acad. Sci. U. S. A.* 107, 14466–14471. doi:10.1073/pnas.1004243107/-
694 /DCSupplemental.www.pnas.org/cgi/doi/10.1073/pnas.1004243107.

695 Igloi, K., Doeller, C. F., Paradis, A.-L., Benchenane, K., Berthoz, A., Burgess, N., et al.
696 (2015). Interaction Between Hippocampus and Cerebellum Crus I in Sequence-Based but
697 not Place-Based Navigation. *Cereb. Cortex* 25, 4146–4154. doi:10.1093/cercor/bhu132.

698 Igloi, K., Doeller, C. F., Paradis, A.-L., Benchenane, K., Berthoz, A., Burgess, N., et al.
699 (2014). Interaction Between Hippocampus and Cerebellum Crus I in Sequence-Based but
700 not Place-Based Navigation. *Cereb. Cortex*, bhu132-. doi:10.1093/cercor/bhu132.

701 Ito, H. T. (2018). Prefrontal-hippocampal interactions for spatial navigation. *Neurosci. Res.*
702 129, 2–7. doi:10.1016/j.neures.2017.04.016.

703 Janzen, G., and van Turennout, M. (2004). Selective neural representation of objects relevant
704 for navigation. *Nat. Neurosci.* 7, 673–677. doi:10.1038/nn1257.

705 Javadi, A.-H., Emo, B., Howard, L. R., Zisch, F. E., Yu, Y., Knight, R., et al. (2017).
706 Hippocampal and prefrontal processing of network topology to simulate the future. *Nat.*
707 *Commun.* 8, 14652. doi:10.1038/ncomms14652.

708 Julian, J. B., Keinath, A. T., Marchette, S. A., and Epstein, R. A. (2018). The Neurocognitive
709 Basis of Spatial Reorientation. *Curr. Biol.* 28, R1059–R1073.
710 doi:10.1016/j.cub.2018.04.057.

711 Julian, J. B., Ryan, J., Hamilton, R. H., Epstein, R. A., Julian, J. B., Ryan, J., et al. (2016).
712 The Occipital Place Area Is Causally Involved in Representing Environmental
713 Boundaries during Navigation. *Curr. Biol.*, 1–6. doi:10.1016/j.cub.2016.02.066.

714 Kamps, F. S., Julian, J. B., Kubilius, J., Kanwisher, N., and Dilks, D. D. (2016). The occipital
715 place area represents the local elements of scenes. *Neuroimage* 132, 417–424.
716 doi:10.1016/j.neuroimage.2016.02.062.

717 Kauffmann, L., Ramanoël, S., and Peyrin, C. (2014). The neural bases of spatial frequency
718 processing during scene perception. *Front. Integr. Neurosci.* 8.
719 doi:10.3389/fnint.2014.00037.

720 Kimura, K., Reichert, J. F., Kelly, D. M., and Moussavi, Z. (2019). Older Adults Show Less
721 Flexible Spatial Cue Use When Navigating in a Virtual Reality Environment Compared

With Younger Adults. *Neurosci. Insights* 14, 2633105519896803. doi:10.1177/2633105519896803.

Kirasic, K. C. (1991). Spatial cognition and behavior in young and elderly adults: implications for learning new environments. *Psychol. Aging* 6, 10–18. doi:10.1037//0882-7974.6.1.10.

Konishi, K., Etchamendy, N., Roy, S., Marighetto, A., Rajah, N., and Bohbot, V. D. (2013). Decreased functional magnetic resonance imaging activity in the hippocampus in favor of the caudate nucleus in older adults tested in a virtual navigation task. *Hippocampus* 23, 1005–1014. doi:10.1002/hipo.22181.

Kozhevnikov, M., and Hegarty, M. (2001). A dissociation between object manipulation spatial ability and spatial orientation ability. *Mem. Cognit.* 29, 745–756. doi:10.3758/bf03200477.

Kozhevnikov, M., Motes, M. A., Rasch, B., and Blajenkova, O. (2006). Perspective-taking vs. mental rotation transformations and how they predict spatial navigation performance. *Appl. Cogn. Psychol.* 20, 397–417. doi:10.1002/acp.1192.

Kravitz, D. J., Saleem, K. S., Baker, C. I., Ungerleider, L. G., and Mishkin, M. (2013). The ventral visual pathway: an expanded neural framework for the processing of object quality. *Trends Cogn. Sci.* 17, 26–49. doi:https://doi.org/10.1016/j.tics.2012.10.011.

Kuhn, S., and Gallinat, J. (2014). Segregating cognitive functions within hippocampal formation: a quantitative meta-analysis on spatial navigation and episodic memory. *Hum. Brain Mapp.* 35, 1129–1142. doi:10.1002/hbm.22239.

Laczo, J., Andel, R., Nedelska, Z., Vyhnalek, M., Vlcek, K., Crutch, S., et al. (2017). Exploring the contribution of spatial navigation to cognitive functioning in older adults. *Neurobiol. Aging* 51, 67–70. doi:10.1016/j.neurobiolaging.2016.12.003.

Laczo, J., Parizkova, M., and Moffat, S. D. (2018). Spatial navigation, aging and Alzheimer's disease. *Aging (Albany. NY).* 10, 3050–3051. doi:10.18632/aging.101634.

Lester, A. W., Moffat, S. D., Wiener, J. M., Barnes, C. A., and Wolbers, T. (2017). The Aging Navigational System. *Neuron* 95, 1019–1035. doi:10.1016/j.neuron.2017.06.037.

Li, A. W. Y., and King, J. (2019). Spatial memory and navigation in ageing: A systematic

751 review of MRI and fMRI studies in healthy participants. *Neurosci. Biobehav. Rev.* 103,
752 33–49. doi:10.1016/j.neubiorev.2019.05.005.

753 Lithfous, S., Dufour, A., and Despres, O. (2013). Spatial navigation in normal aging and the
754 prodromal stage of Alzheimer's disease: insights from imaging and behavioral studies.
755 *Ageing Res. Rev.* 12, 201–213. doi:10.1016/j.arr.2012.04.007.

756 Litman, L., Awipi, T., and Davachi, L. (2009). Category-specificity in the human medial
757 temporal lobe cortex. *Hippocampus* 19, 308–319. doi:10.1002/hipo.20515.

758 Marchette, S. a, Vass, L. K., Ryan, J., and Epstein, R. a (2015). Outside Looking In:
759 Landmark Generalization in the Human Navigational System. *J. Neurosci.* 35, 14896–
760 908. doi:10.1523/JNEUROSCI.2270-15.2015.

761 Mazaika, P.; Hoeft, F.; Glover, GH.; Reiss, A. . (2009). Methods and Software for fMRI
762 analysis for Clinical Subjects. in *Organization for Human Brain Mapping* (San
763 Francisco, CA, USA).

764 Meneghetti, C., Muffato, V., Borella, E., and De Beni, R. (2018). Map Learning in Normal
765 Aging: The Role of Individual Visuo-Spatial Abilities and Implications. *Curr.*
766 *Alzheimer Res.* 15, 205–218. doi:10.2174/1567205014666171030113515.

767 Merhav, M., Riemer, M., and Wolbers, T. (2019). Spatial updating deficits in human aging
768 are associated with traces of former memory representations. *Neurobiol. Aging* 76, 53–
769 61. doi:10.1016/j.neurobiolaging.2018.12.010.

770 Merhav, M., and Wolbers, T. (2019). Aging and spatial cues influence the updating of
771 navigational memories. *Sci. Rep.* 9, 11469. doi:10.1038/s41598-019-47971-2.

772 Meulenbroek, O., Petersson, K. M., Voermans, N., Weber, B., and Fernandez, G. (2004). Age
773 differences in neural correlates of route encoding and route recognition. *Neuroimage* 22,
774 1503–1514. doi:10.1016/j.neuroimage.2004.04.007.

775 Miniaci, M. C., and De Leonibus, E. (2018). Missing the egocentric spatial reference: a blank
776 on the map. *F1000Research* 7, 168. doi:10.12688/f1000research.13675.1.

777 Mitchell, A. S., Czajkowski, R., Zhang, N., Jeffery, K., and Nelson, A. J. D. (2018).
778 Retrosplenial cortex and its role in spatial cognition. *Brain Neurosci. Adv.* 2,
779 2398212818757098. doi:10.1177/2398212818757098.

780 Moffat, S. D. (2009). Aging and spatial navigation: What do we know and where do we go?
781 *Neuropsychol. Rev.* 19, 478–489. doi:10.1007/s11065-009-9120-3.

782 Moffat, S. D., Elkins, W., and Resnick, S. M. (2006). Age differences in the neural systems
783 supporting human allocentric spatial navigation. *Neurobiol. Aging* 27, 965–972.
784 doi:10.1016/j.neurobiolaging.2005.05.011.

785 Moffat, S. D., and Resnick, S. M. (2002). Effects of age on virtual environment place
786 navigation and allocentric cognitive mapping. *Behav. Neurosci.* 116, 851–859.
787 doi:10.1037/0735-7044.116.5.851.

788 Muffato, V., Meneghetti, C., and De Beni, R. (2020). The role of visuo-spatial abilities in
789 environment learning from maps and navigation over the adult lifespan. *Br. J. Psychol.*
790 111, 70–91. doi:10.1111/bjop.12384.

791 Nau, M., Julian, J. B., and Doeller, C. F. (2018). How the Brain's Navigation System Shapes
792 Our Visual Experience. *Trends Cogn. Sci.* 22, 810–825. doi:10.1016/j.tics.2018.06.008.

793 Ohta, R. J., Walsh, D. A., and Krauss, I. K. (1981). Spatial perspective-taking ability in young
794 and elderly adults. *Exp. Aging Res.* 7, 45–63. doi:10.1080/03610738108259785.

795 Packard, M. G., and Goodman, J. (2013). Factors that influence the relative use of multiple
796 memory systems. *Hippocampus* 23, 1044–1052. doi:10.1002/hipo.22178.

797 Perrochon, A., Mandigout, S., Petruzzellis, S., Soria Garcia, N., Zaoui, M., Berthoz, A., et al.
798 (2018). The influence of age in women in visuo-spatial memory in reaching and
799 navigation tasks with and without landmarks. *Neurosci. Lett.* 684, 13–17.
800 doi:10.1016/j.neulet.2018.06.054.

801 Persichetti, A. S., and Dilks, D. D. (2016). Perceived egocentric distance sensitivity and
802 invariance across scene-selective cortex. *Cortex.* 77, 155–163.
803 doi:10.1016/j.cortex.2016.02.006.

804 Persichetti, A. S., and Dilks, D. D. (2018). Dissociable Neural Systems for Recognizing
805 Places and Navigating through Them. *J. Neurosci.* 38, 10295 LP – 10304.
806 doi:10.1523/JNEUROSCI.1200-18.2018.

807 Persichetti, A. S., and Dilks, D. D. (2019). Distinct representations of spatial and categorical
808 relationships across human scene-selective cortex. *Proc. Natl. Acad. Sci.* 116, 21312 LP

809 – 21317. doi:10.1073/pnas.1903057116.

810 Picucci, L., Caffò, A. O., and Bosco, A. (2009). Age and sex differences in a virtual version
811 of the reorientation task. *Cogn. Process.* doi:10.1007/s10339-009-0321-8.

812 Ramanoël, S., Kauffmann, L., Cousin, E., Dojat, M., and Peyrin, C. (2015). Age-related
813 differences in spatial frequency processing during scene categorization. *PLoS One*.
814 doi:10.1371/journal.pone.0134554.

815 Ramanoël, S., York, E., Le Petit, M., Lagrene, K., Habas, C., and Arleo, A. (2019). Age-
816 Related Differences in Functional and Structural Connectivity in the Spatial Navigation
817 Brain Network. *Front. Neural Circuits* 13, 69. doi:10.3389/fncir.2019.00069.

818 Ratliff, K. R., and Newcombe, N. S. (2008). Reorienting when cues conflict: Evidence for an
819 adaptive-combination view. *Psychol. Sci.* doi:10.1111/j.1467-9280.2008.02239.x.

820 Rochefort, C., Lefort, J. M., and Rondi-Reig, L. (2013). The cerebellum: a new key structure
821 in the navigation system. *Front. Neural Circuits* 7, 35. doi:10.3389/fncir.2013.00035.

822 Rodgers, M. K., Sindone, J. A., and Moffat, S. D. (2012). Effects of age on navigation
823 strategy. *Neurobiol. Aging* 33, 202.e15-202.e22.
824 doi:10.1016/j.neurobiolaging.2010.07.021.

825 Sack, A. T. (2009). Parietal cortex and spatial cognition. *Behav. Brain Res.* 202, 153–161.
826 doi:https://doi.org/10.1016/j.bbr.2009.03.012.

827 Schuck, N. W., Doeller, C. F., Polk, T. A., Lindenberger, U., and Li, S.-C. (2015a). Human
828 aging alters the neural computation and representation of space. *Neuroimage* I, 141–150.
829 doi:10.1016/j.neuroimage.2015.05.031.

830 Schuck, N. W., Doeller, C. F., Polk, T. A., Lindenberger, U., and Li, S. C. (2015b). Human
831 aging alters the neural computation and representation of space. *Neuroimage*.
832 doi:10.1016/j.neuroimage.2015.05.031.

833 Seghier, M. L. (2012). The Angular Gyrus. *Neurosci.* 19, 43–61.
834 doi:10.1177/1073858412440596.

835 Sherrill, K. R., Chrastil, E. R., Ross, R. S., Erdem, U. M., Hasselmo, M. E., and Stern, C. E.
836 (2015). Functional connections between optic flow areas and navigationally responsive

837 brain regions during goal-directed navigation. *Neuroimage* 118, 386–396.
838 doi:10.1016/j.neuroimage.2015.06.009.

839 Spiers, H. J., and Barry, C. (2015a). Neural systems supporting navigation. *Curr. Opin.*
840 *Behav. Sci.* 1, 47–55. doi:10.1016/j.cobeha.2014.08.005.

841 Spiers, H. J., and Barry, C. (2015b). Neural systems supporting navigation. *Curr. Opin.*
842 *Behav. Sci.* 1, 47–55. doi:https://doi.org/10.1016/j.cobeha.2014.08.005.

843 Stankiewicz, B. J., and Kalia, A. A. (2007). Acquisition of Structural Versus Object
844 Landmark Knowledge. *J. Exp. Psychol. Hum. Percept. Perform.* doi:10.1037/0096-
845 1523.33.2.378.

846 Sturz, B. R., Kilday, Z. A., and Bodily, K. D. (2013). Does constraining field of view prevent
847 extraction of geometric cues for humans during virtual-environment reorientation? *J.*
848 *Exp. Psychol. Anim. Behav. Process.* 39, 390–396. doi:10.1037/a0032543.

849 Sutton, J. E., Joanisse, M. F., and Newcombe, N. S. (2010). Spinning in the scanner: Neural
850 correlates of virtual reorientation. *J. Exp. Psychol. Learn. Mem. Cogn.* 36, 1097–1107.
851 doi:10.1037/a0019938.

852 Techentin, C., Voyer, D., and Voyer, S. D. (2014). Spatial Abilities and Aging: A Meta-
853 Analysis. *Exp. Aging Res.* 40, 395–425. doi:10.1080/0361073X.2014.926773.

854 Tommasi, L., Chiandetti, C., Pecchia, T., Sovrano, V. A., and Vallortigara, G. (2012). From
855 natural geometry to spatial cognition. *Neurosci. Biobehav. Rev.* 36, 799–824.
856 doi:10.1016/j.neubiorev.2011.12.007.

857 United Nations, Departement of Economic and Social Affairs, Population Division (2019).
858 World population ageing. Highlight (ST/ESA/SER.A/430).

859 van der Ham, I. J. M., Baalbergen, H., van der Heijden, P. G. M., Postma, A., Braspenning,
860 M., and van der Kuil, M. N. A. (2015). Distance comparisons in virtual reality: effects of
861 path, context, and age. *Front. Psychol.* 6, 1103. doi:10.3389/fpsyg.2015.01103.

862 van der Ham, I. J. M., and Claessen, M. H. G. (2020). How age relates to spatial navigation
863 performance: Functional and methodological considerations. *Ageing Res. Rev.* 58,
864 101020. doi:https://doi.org/10.1016/j.arr.2020.101020.

865 Vandenberg, S. G., and Kuse, A. R. (1978). Mental rotations, a group test of three-
866 dimensional spatial visualization. *Percept. Mot. Skills* 47, 599–604.
867 doi:10.2466/pms.1978.47.2.599.

868 Vann, S. D., Aggleton, J. P., and Maguire, E. A. (2009). What does the retrosplenial cortex
869 do? *Nat. Rev. Neurosci.* 10, 792–802. doi:10.1038/nrn2733.

870 Wandell, B. A., Brewer, A. A., and Dougherty, R. F. (2005). Visual field map clusters in
871 human cortex. *Philos. Trans. R. Soc. Lond. B. Biol. Sci.* 360, 693–707.
872 doi:10.1098/rstb.2005.1628.

873 Weiskopf, N., Hutton, C., Josephs, O., and Deichmann, R. (2006). Optimal EPI parameters
874 for reduction of susceptibility-induced BOLD sensitivity losses: A whole-brain analysis
875 at 3 T and 1.5 T. *Neuroimage*. doi:10.1016/j.neuroimage.2006.07.029.

876 Wiener, J. M., de Condappa, O., Harris, M. A., and Wolbers, T. (2013). Maladaptive Bias for
877 Extrahippocampal Navigation Strategies in Aging Humans. *J. Neurosci.*
878 doi:10.1523/jneurosci.0717-12.2013.

879 Wiener, J. M., Kmecova, H., and de Condappa, O. (2012). Route repetition and route
880 retracing: Effects of cognitive aging. *Front. Aging Neurosci.* 4, 1–7.
881 doi:10.3389/fnagi.2012.00007.

882 Wilkniss, S. M., Jones, M. G., Korol, D. L., Gold, P. E., and Manning, C. A. (1997). Age-
883 related differences in an ecologically based study of route learning. *Psychol. Aging* 12,
884 372–375. doi:10.1037/0882-7974.12.2.372.

885 Wolbers, T., and Büchel, C. (2005). Dissociable Retrosplenial and Hippocampal
886 Contributions to Successful Formation of Survey Representations. *J. Neurosci.* 25,
887 3333–3340. doi:10.1523/JNEUROSCI.4705-04.2005.

888 Wolbers, T., and Hegarty, M. (2010). What determines our navigational abilities? *Trends*
889 *Cogn. Sci.* 14, 138–146. doi:10.1016/j.tics.2010.01.001.

890 Zajac, L., Burte, H., Taylor, H. A., and Killiany, R. (2019). Self-reported navigation ability is
891 associated with optic flow-sensitive regions' functional connectivity patterns during
892 visual path integration. *Brain Behav.* 9, e01236. doi:10.1002/brb3.1236.

893 Zhong, J. Y., and Moffat, S. D. (2016). Age-Related Differences in Associative Learning of

894 Landmarks and Heading Directions in a Virtual Navigation Task. *Front. Aging Neurosci.*
895 8, 122. doi:10.3389/fnagi.2016.00122.

896 Zhong, J. Y., and Moffat, S. D. (2018). Extrahippocampal Contributions to Age-Related
897 Changes in Spatial Navigation Ability. *Front. Hum. Neurosci.* 12, 272.
898 doi:10.3389/fnhum.2018.00272.

899

	Groups		
	Young adults	**Older adults**	
Sex (M/F)	**18/7**	**7/10**	
	Mean (± SEM)	**Mean (± SEM)**	**p-value**
Age[1]	25.4 (± 0.5)	73.0 (± 0.9)	$p < 0.001$
Total brain volume[1] (cm^3)	1301 (± 18)	1061 (± 23)	$p < 0.001$
MMSE[2]	30.0 (± 0.0)	28.8 (± 0.4)	$p < 0.001$
3D mental rotation[1]	18.3 (± 0.9)	12.7 (± 1.2)	$p < 0.001$
Corsi forward[2]	7.2 (± 0.2)	4.4 (± 0.2)	$p < 0.001$
Corsi backward[2]	6.2 (± 0.3)	4.6 (± 0.2)	$p < 0.001$
Perspective taking test[2]	15.3 (± 1.7)	46.1 (± 6.7)	$p < 0.001$

Table 1. Descriptive characteristics and cognitive performance of young and older participants. M: male; F: female; SEM: standard error of the mean; MMSE: mini mental state examination; [1]Independent samples t-test; [2]Mann Whitney U test.

		H	BA	k	x	y	z	t
Multiple Regression Navigation time / [Landmark > Control]								
All participants	Inferior Temporal Gyrus	R	21	40	45	-22	-16	5.17
					51	-28	-7	4.56
	Middle Frontal Gyrus	R	9	35	18	44	26	4.91
	Middle Temporal Gyrus	R	20	16	45	8	-37	4.84
					54	5	-34	4.04
	Lingual Gyrus	R	-	15	30	-49	2	4.66
	[Middle Temporal Gyrus]				42	-49	5	3.65
	Lingual Gyrus	L	-	22	-24	-46	5	4.58
	Angular Gyrus	L	39	76	-57	-58	29	4.54
					-54	-70	26	4.41
					-45	-79	35	3.99
	Cerebellum Lobule VI	R	-	10	15	-67	-28	4.48
				15	27	-55	-31	4.38
	Superior Occipital Gyrus	L	18	14	-21	-97	23	4.41
	Cerebellum Vermis			58	0	-55	-4	4.35
					0	-40	-13	3.91
	Parahippocampal Gyrus	L	-	19	-36	-43	-4	4.17
					-36	-34	-10	3.61
	Superior Frontal Gyrus	R	10	20	9	62	23	4.03
					6	68	14	3.60
Young adults	Superior Frontal Gyrus	L		13	-15	11	44	4.52
	Precentral Gyrus	R		11	9	-22	77	4.16
Older adults	Angular Gyrus	L		20	-60	-55	29	5.84
	Brainstem / Parahippocampal Gyrus	L		12	-3	-34	-7	4.90

Table 2. Cerebral regions whose activity for the contrast [Landmark > Control] was predicted by navigation time across all participants and across age groups (sex and intracranial volume were included as covariates). The statistical threshold was defined as $p < 0.001$ uncorrected for multiple comparisons at voxel-level with an extent voxel threshold set at 10 voxels. For each cluster, the region with the maximum t-value is listed first and other regions in the cluster are listed underneath [in square brackets]. Montreal Neurological Institute (MNI) coordinates (x, y, z) of the peak activation and number of voxels (k) in a cluster are also shown. H = hemisphere; R = right hemisphere; L = left hemisphere; BA = Brodmann area.

		H	BA	k	x	y	z	t
Group Analyses [Landmark > Control]								
Within group								
[Young]	Inferior Occipital Gyrus	R	18	65	30	-88	-10	5.07
	Superior Temporal Gyrus	L	38	21	-48	20	-25	4.54
					-42	11	-22	4.01
	Cerebellum Crus I-II	R	-	19	33	-82	-34	4.49
	Middle Occipital Gyrus	L	18	37	-30	-97	-7	4.42
	[Inferior Occipital Gyrus]	L	19		-39	-85	-13	3.54
	Inferior Temporal Gyrus (Amygdala / Hippocampus)	L	53/54	15	-30	-1	-22	4.37
	Middle Occipital Gyrus	R	19	16	48	-79	2	4.20
[Old]	*No significant activation*							
Between group								
[Young > Old]	Inferior Temporal Gyrus (Amygdala / Hippocampus)	L	-	12	-33	2	-25	3.86
					-36	-7	-25	3.82
[Old> Young]	*No significant activation*							

Table 3. Cerebral regions whose activity for the contrast [Landmark > Control] was elicited by within-group or between-group analyses (total intracranial volume was included as a covariate). The statistical threshold was defined as $p < 0.001$ uncorrected for multiple comparisons at voxel-level with an extent voxel threshold set at 10 voxels. For each cluster, the region with the maximum t-value is listed first and other regions in the cluster are listed underneath [in square brackets]. Montreal Neurological Institute (MNI) coordinates (x, y, z) of the peak activation and number of voxels (k) in a cluster are also shown. H = hemisphere; R = right hemisphere; L = left hemisphere; BA = Brodmann area.

		H	BA	k	x	y	z	t
Group Analyses [CTRL > Fix]								
[Young > Old]	*No significant activation*							
[Old > Young]	Middle Frontal Gyrus	L	8	80	-27	32	56	5.56
	[Middle Frontal Gyrus]				-36	23	56	4.58
	[Superior Frontal Gyrus]		6		-18	32	62	4.05
	Superior Temporal Gyrus	R	-	18	36	17	-19	4.71
	Superior Frontal Gyrus	R	10	32	12	56	-10	4.56
	[Middle Frontal Gyrus]				15	44	-4	4.02
	Inferior Temporal Gyrus	L	37	25	-54	-49	-13	4.39
	Supramarginal Gyrus	R	40	31	42	-40	41	4.23
	[Superior Parietal Gyrus]		7		33	-46	38	4.21
	Superior Frontal Gyrus	L	32	14	-12	41	2	4.16
	[Middle Frontal Gyrus]				-18	41	-4	4.10
	Inferior Frontal Gyrus	L	46	38	-36	35	14	4.15
					-48	41	11	3.85
	Precuneus	R	31	12	9	-58	38	4.00
	Middle Frontal Gyrus	L	8	20	-51	20	41	3.92
					-48	11	50	3.81
	Inferior Frontal Gyrus	L	45	12	-57	23	8	3.79

Table 4. Cerebral regions whose activity for the contrast [Control > Fixation] was elicited by between-group analyses (total intracranial volume was included as covariate). The statistical threshold was defined as $p < 0.001$ uncorrected for multiple comparisons at voxel-level with an extent voxel threshold set at 10 voxels. For each cluster, the region with the maximum t-value is listed first and other regions in the cluster are listed underneath [in square brackets]. Montreal Neurological Institute (MNI) coordinates (x, y, z) of the peak and number of voxels (k) of clusters are also shown. CTRL = Control condition; Fix = Fixation; H = hemisphere; R = right hemisphere; L = left hemisphere; BA = Brodmann area.

		H	BA	k	x	y	z	t
Group Analyses [LMK > Fix]								
[Young > Old]	*No significant activation*							
[Old > Young]	Middle Frontal Gyrus	R		22	24	47	-1	6.06
	Angular Gyrus	L		223	-30	-64	47	5.66
	[Superior Parietal Gyrus]				-33	-55	44	5.59
	[Supramarginal Gyrus]				-48	-43	44	5.32
	Middle Frontal Gyrus	R		34	39	38	17	5.37
					33	47	20	4.47
	Cerebellum	R	-	23	36	-73	-22	5.19
	Middle Frontal Gyrus	L		127	-42	5	41	5.14
					-45	26	26	5.13
					-45	5	50	5.12
	Superior Parietal Gyrus	R		36	30	-55	44	4.89
	[Angular Gyrus]				30	-64	53	4.64

Table 5. Cerebral regions whose activity for the contrast [Landmark > Fixation] was elicited by between-group analyses (total intracranial volume was included as covariate). The statistical threshold for cluster was defined as $p < 0.05$ FWE-corrected for multiple comparisons with an extent voxel threshold set at 10 voxels. For each cluster, the region with the maximum t-value is listed first and other regions in the cluster are listed underneath [in square brackets]. Montreal Neurological Institute (MNI) coordinates (x, y, z) of the peak and number of voxels (k) of clusters are also shown. LMK = Landmark condition; Fix: Fixation condition; H = hemisphere; R = right hemisphere; L = left hemisphere; BA = Brodmann area; FWE = family-wise error.

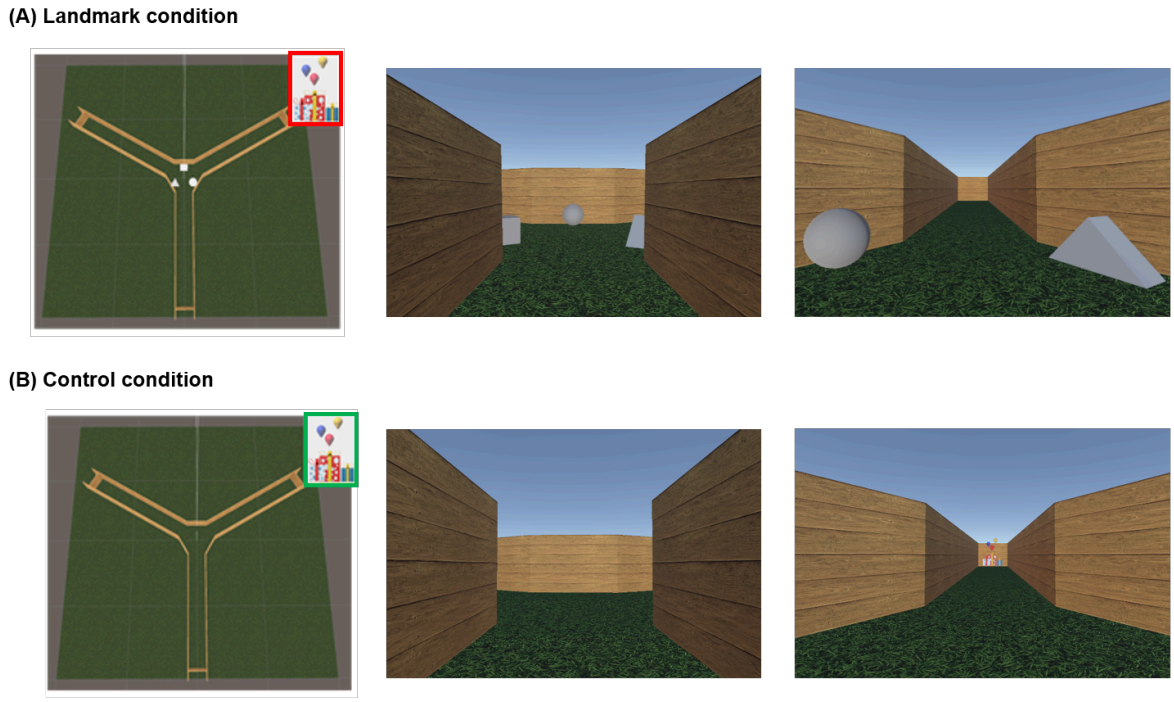

946

947 **Figure 1.** The virtual environment. **(A)** An overhead perspective of the environment for the
948 landmark condition and two example views representing a first-person perspective within the
949 maze. **(B)** An overhead perspective of the environment for the control condition and example
950 views within the maze. Red: hidden goal; Green: visible goal. The aerial view was never seen
951 by participants.

952

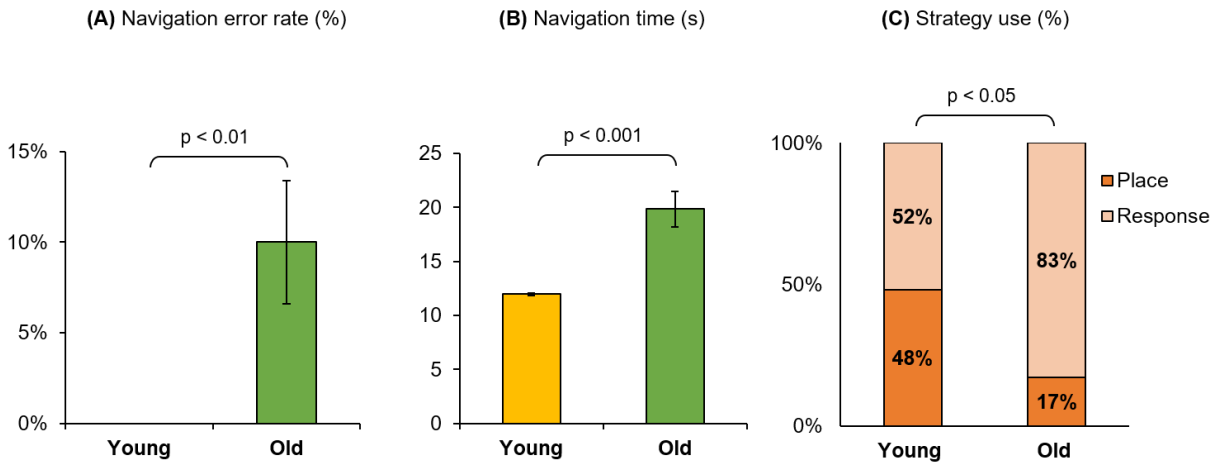

953

954 **Figure 2.** Behavioral results for the virtual navigation task across age groups. **(A)** Proportion
955 of trials in which the wrong corridor was chosen (navigation error rate). **(B)** Time taken to
956 reach the goal averaged across 7 trials in the landmark condition (navigation time). **(C)**
957 Proportion of participants who used a place-based or response-based strategy in the landmark
958 condition (strategy use). Error bars represent the standard errors of the mean.

959

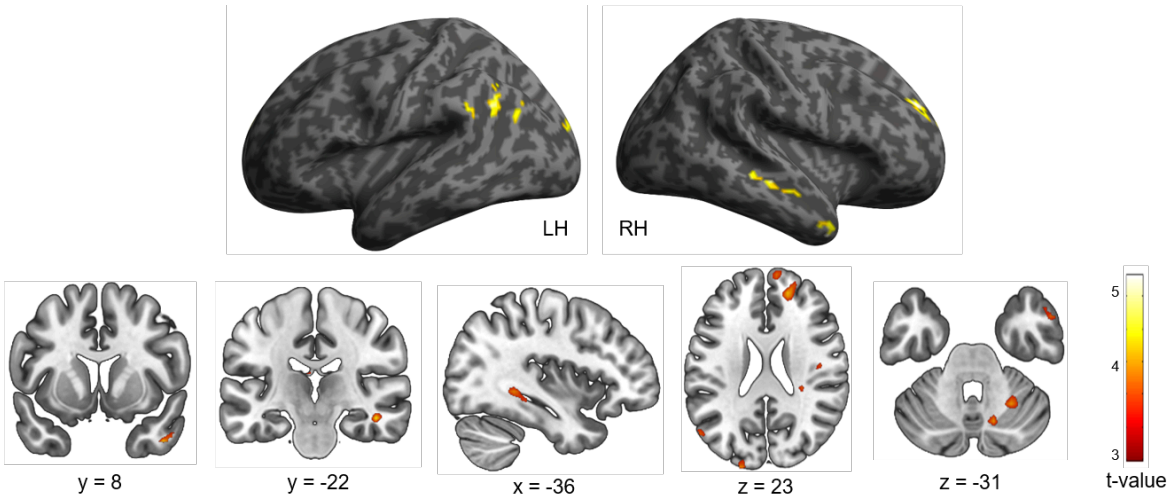

Figure 3. Cerebral regions whose activity for the contrast [Landmark > Control] was predicted by navigation time projected onto 3D inflated anatomical templates and 2D slices ($p < 0.001$ uncorrected, k = 10 voxels). LH: left hemisphere; RH: right hemisphere.

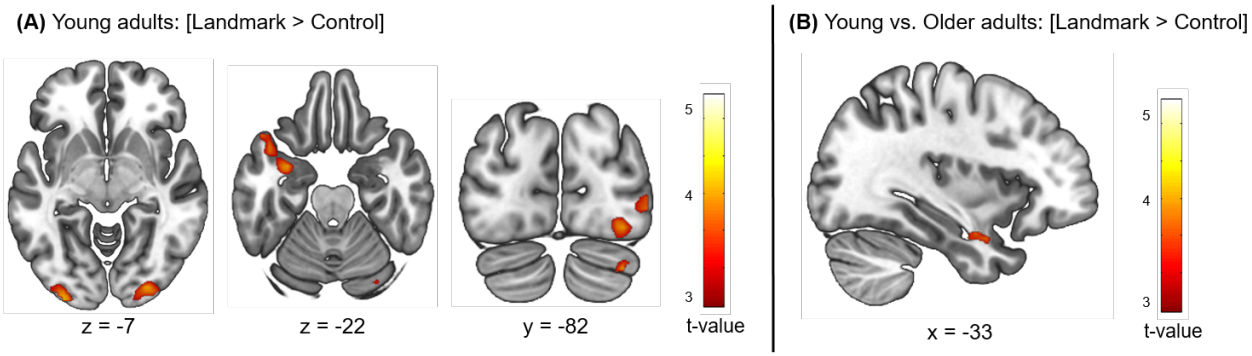

965

966 **Figure 4**. Cerebral regions whose activity for the contrast [Landmark > Control] was elicited
967 by within- **(A)** or between-group **(B)** analyses projected onto 2D slices ($p < 0.001$
968 uncorrected, k = 10 voxels).

969

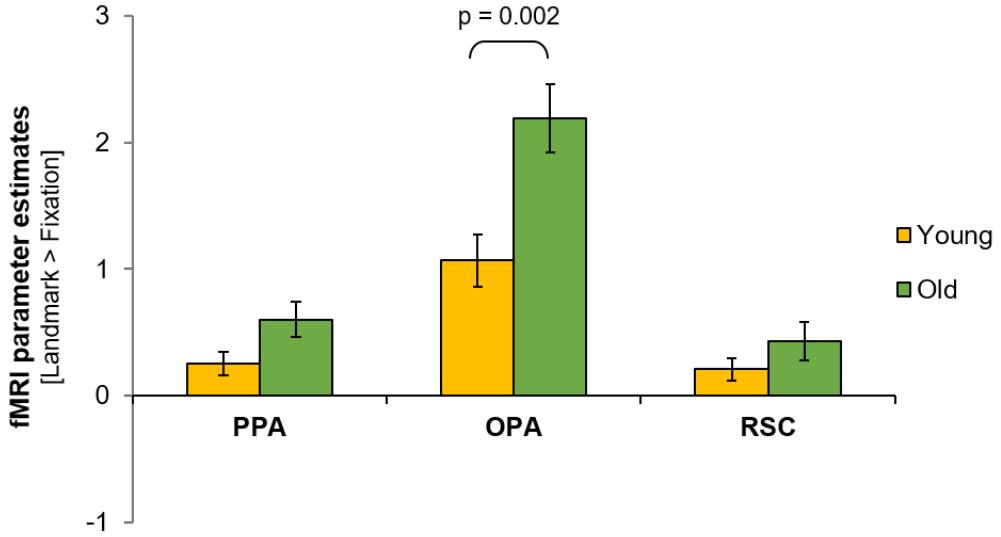

970

971 **Figure 5**. FMRI parameter estimates in the PPA, OPA, and RSC for the fMRI contrast
972 [Landmark > Fixation] across age groups. Error bars reflect standard errors of the mean.

973

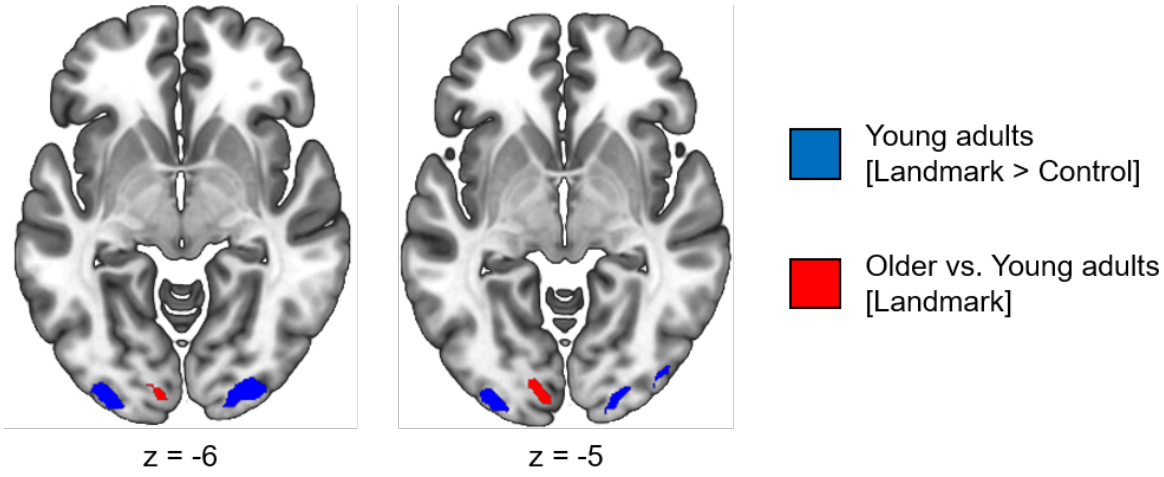

Figure 6. Occipital clusters recruited during the navigation task. In blue, the cortical projection of the central visual field that was elicited by the fMRI contrast [Landmark > Control] in young adults. In red, the cortical projection of the peripheral visual field that was elicited by comparing young and older adults for the fMRI contrast [Landmark].